Lasers in Manufacturing Conference 2019

Increasing Productivity of Selective Laser Sintering with beam shaping

Steffen Boley[a*], Alexander Peter[a], Volkher Onuseit[a], Thomas Graf[a]

[a]*Institut für Strahlwerkzeuge (IFSW), University of Stuttgart, Pfaffenwaldring 43, 70569 Stuttgart, Germany*

Abstract

Productivity of additive manufacturing processes like Selective Laser sintering Sintering (SLS) is mainly driven by the usable laser power, which is limited by the process itself. A common way to scale the power is to increase the number of spots, or scaling the spot in size by defocusing, which results in lower printing resolution. In this work, we will present a scaling of the illumination area without loss of resolution with a spatial light modulator as beam shaping optic. The beam intensity profile can be adjusted dynamically to the illumination area, which allows us to increase and decrease the spot size from 100 µm² to five mm². With this approach, the usable laser power increases by a factor of five compared to conventional single spot processing parameters. The experiments showed no warping at single layer processing and promise good printing results.

Keywords: Additive Manufacturing, Selective Laser Sintering

1. Introduction

The usable laser power per volume in Selective Laser Sintering (SLS) is limited due to the materials' printing temperature interval as shown in (Peyre et al. 2015). If the material is heated above a specific temperature, a loss in printing quality, like thermal degradation of the material or distortions, is observed. The working temperature is limited to a small temperature range between the melting point and the crystallization temperature. Therefore, the process window is very small and the right energy input is necessary to get a good printing result. As shown in (Paul und Anand 2012), the applicable beam intensity on

* Corresponding author. Tel.: +49-711-685-66823.
E-mail address: steffen.boley@ifsw.uni-stuttgart.de.

the powder surface is limited and depends on the scan speed due to the thermal conductivity of the powder. Besides depending on preheating, coating and cool down of the printed workpiece, the productive printing time is a function of the sintered volume per time. Because of the intensity limit and the given sintering depth, the productivity can only be increased by an enlarged illumination area. To maximize the illuminated area per time without overheating the surface with high beam intensities, it is necessary to scale the beam size by e.g. defocusing or beam shaping. Beam shaping with static diffractive optic elements is possible but inflexible when illuminating different geometries. This contradicts the freedom of 3D printing. For this reason, a spatial light modulator was utilized in this work to shape the beam to different profiles. The setup was used to print single layers of PA 12 black with high and low energy distribution and beam intensities.

2. Experimental Setup

2.1. Material and Assessment Criteria

PA 12 black powder is a common SLS printing material used in combination with diode and solid state lasers. To increase the absorptivity for near infrared and visible wavelength lasers, standard PA12 plastic powder is mixed with carbon black. The higher absorptivity allows the usage of shorter wavelengths and therefore the use of transport fibers and fused silica glass as well as dynamic beam shaping optics such as a spatial light modulator. The thermal properties of the material are very important for the printing process. The glass transition temperature (~ 176 °C) of PA 12 and the much lower crystallization temperature (~ 149 °C) represent the process window for this material.

In this work, productivity of SLS printing is defined as volume printed per time including positioning and jump times of the used galvanometer scanner. As assessment criteria for a single layer print, the melted depth and the surface quality in grey scale were used. The melted depth represents the energy transformed to molten material while the surface quality represents deposited energy on the surface and correlates with the beam intensity in combination with the energy input. The melted depth was measured with a sliding caliper. The surface quality was assessed by visual inspection with a scale from 1 to 9 as shown in Fig. 1. Starting from values 1 to 3, the surface consists of small melted areas with almost no melted powder particles in between, leading to a light grey surface. Values 4 to 6 show good print quality in darker grey and represent good printing quality. Values 7 to 9 are nearly black with thermal degraded material and show a warping effect.

Fig. 1. *Visual inspection of the surface quality*, left to right 1 to 9 (1-3 low energy input, 4-6 good quality, 7-9 high energy input)

2.2. Laser Optic and Scanner

The schematic optic setup is shown Fig. 2. As laser source a 1030 nm TruDisk 8001 with a 100 µm Fiber was used. By means of a collimation lens of 100mm focal length and Galilei telescope, the beam diameter was brought to a diameter of 10mm. Due to the unpolarized state of the laser, a thin film polarizer (tfp 1) and beam dump (dump 1) was used to get linear polarization for the modulation of the wave front with the spatial light modulator. For laser power adjustment, an automatically rotatable λ/2-plate and a second tfp and second dump was deployed (tfp 2 and dumb 2).

The beam was modulated by a Hamamatsu X13139-03 SLM to shape the beam profile at the powder bed in a target manner. The 1:1 telescope after the modulator, consisting of two lenses, was used to block the disturbing zero order of the modulated beam at the intermediate focus. Finally, the beam was guided through a galvanometer scanner and an F-Theta lens with a focal length of 163 mm to the powder bed.

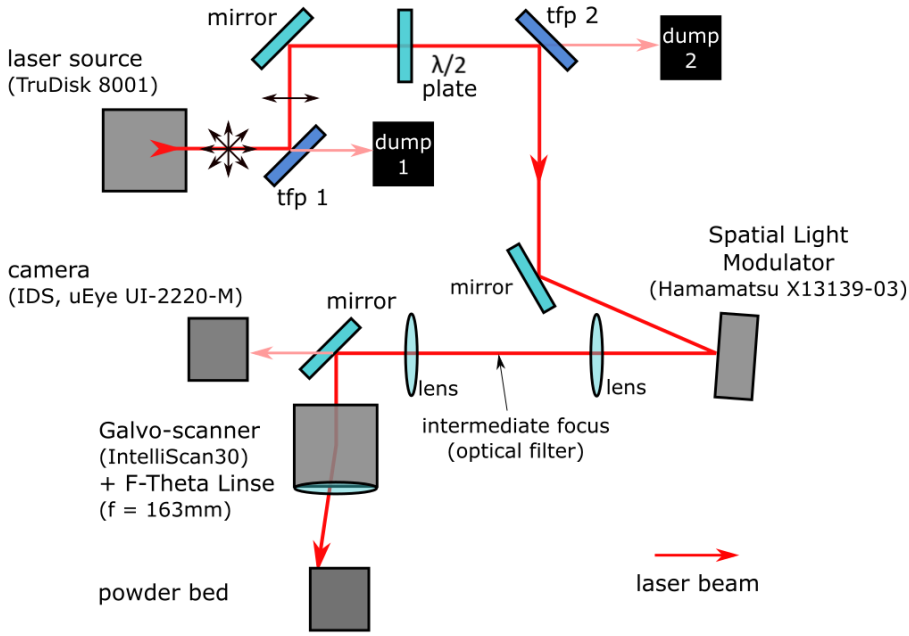

Fig. 2. *Optic setup*

2.3. Spatial Light Modulator and Beam Shaping

In the laser sintering experiments, the results of a line beam profile were compared with a conventional Gaussian beam profile. To reach the conventional diameter of 0.4 mm diameter Gaussian profile, the defocusing phase hologram *H* was calculated by

$$H = c \cdot (x^2 + y^2), \tag{1}$$

where c is a constant that influences the diameter of the resulting beam diameter, and x and y are the pixels of the SLM chip.

The phase hologram for a line with constant intensity distribution was calculated by stretching the top-hat profile from (Dickey Monday 2000),

$$H = \beta_x \phi_x(x) + \beta_y \phi_y(y), \tag{2}$$

with

$$\phi(\xi) = \frac{\sqrt{\pi}}{2}\xi \cdot \mathrm{erf}(\xi) + \frac{1}{2} \cdot \exp(-\xi^2) - \frac{1}{2}, \quad (3)$$

$$\xi = \frac{\sqrt{2} \cdot x}{r_0} \text{ or } \xi = \frac{\sqrt{2} \cdot y}{r_0}, \quad (4)$$

and

$$\beta = \frac{2\sqrt{2\pi} \cdot r_0 y_0}{f\lambda}, \quad (5)$$

with the radius of the incoming Gaussian beam r0 = 1/e2, the half width of the desired rectangular top-hat y0, the focal length of the employed F-Theta lens f and the laser wavelength λ.

E.g. by setting $\beta_y = 0$ and $\beta_x = 9\ \mathrm{mm}$, the resulting beam shape is a line in x direction with the length of 9 mm and the height of the diffraction limit of the laser and optical system. The phase holograms were calculated by MATLAB and written into the spatial light modulator chip via the HDMI interface of the controller. The resulting beam profiles are shown in Fig. 3.

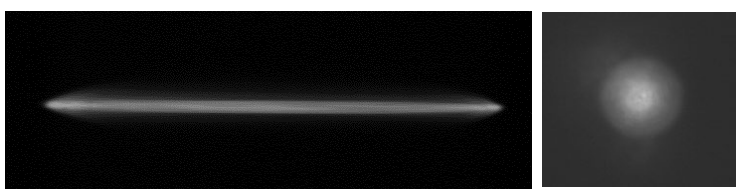

Fig. 3. *Left: 9 mm top-hat beam profile, right: 0.4 mm Gauss beam profile*

As show in Fig. 4 the beam passes the scanner and the focusing f-theta-lens. The generated hologram of the SLM is focused on the surface of the heated powder bed, shown at the bottom.

2.4. Powder Bed and Heating

The powder bed setup is shown in Fig. 4.

The bed is heated by a hot plate made of aluminum to transfer the heat to the powder. Additionally, an 80 W light bulb was placed next to the scanner to heat the top layer. To control the surface temperature, a pyrometer was placed next to the scanner. The bed has a size of 45 mm x 45 mm and a depth of 4 mm. The used powder was Sintratec PA12 Black.

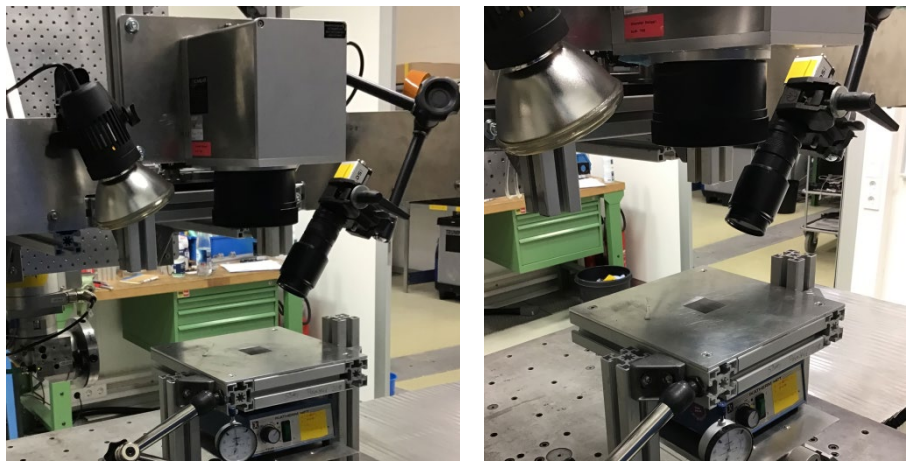

Fig. 4. *Scanner and powder bed (process setup)*

3. Experimental Results

The quality and productivity of the printing process with the two different beam profiles were compared over a range of local intensities and energy inputs per area described in Table 1.

Table 1. Parameters

Parameter	
Powder	PA 12 black
Laser power	2 – 56 W
Scan speed	500 – 9000 mm/s
Bed temperature	160 °C
Gaussian beam diameter	0.4 mm
Rectangle top-hat beam	7 - 9 mm x 0.4 mm
Overlap (Gaussian beam) / Hatching distance	50 % / 0.2 mm
Energy input per area	7 - 23 mJ/mm²
Sample size	10 x 10 mm (SLM line length x 10 mm)

3.1. Gaussian Beam Profile

As reference to shaped beam profile, a conventional Gaussian beam profile with a fixed beam diameter of 0.4 mm was used. The laser power was varied from 2 to 20 W and the scanning velocity was varied from 100 to 9000 mm/s. Different combinations for power and velocity were used to get a variation of the energy per area. Fig. 5 shows the results of the quality rating as defined in Fig. 3. Too low energy per area (< 8 mJ/mm²) leads to loose, not sintered powder with a quality rating ≤ 3. A small window between 10 and 11 mJ/mm

leads to a good quality rating (4 – 6). Higher energy per area leads to a melted surface and warping, and a quality rating of 7 to 9 of a single layer as shown in Fig. 3.

In general, there is a wide range of achieved qualities at a constant level of the energy per area, caused by the different combinations of power and speed, and the different beam intensities.

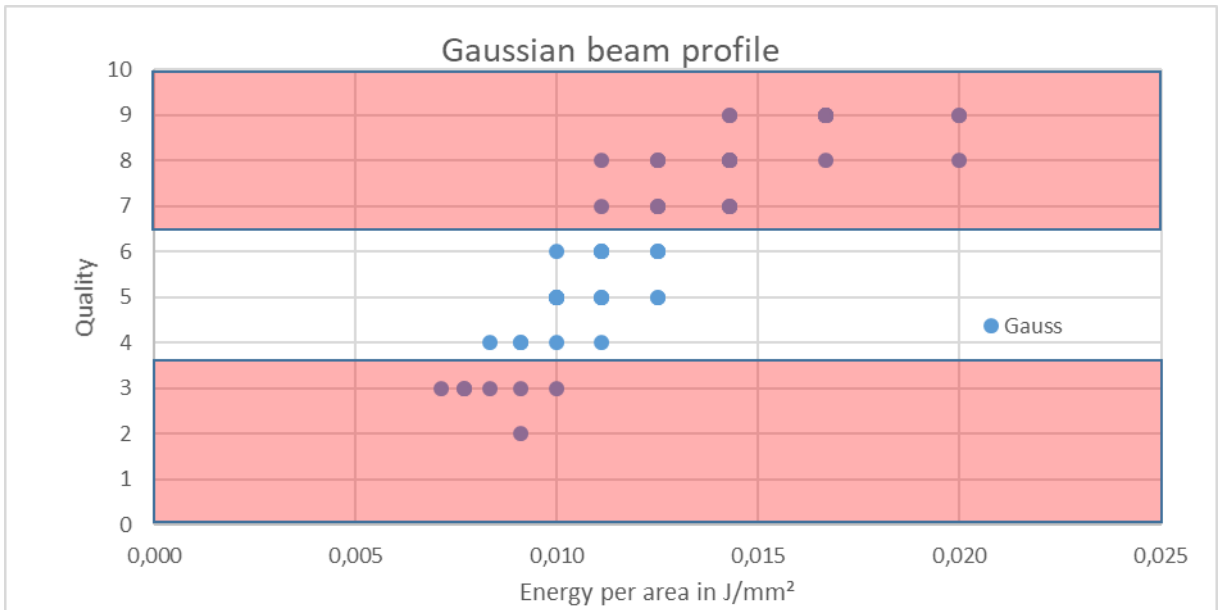

Fig. 5. *Process results: Quality over energy per area*

3.2. Top-hat Beam Profile

In comparison to the quality of the Gaussian beam profile, top-hat line beams with lengths of 9 mm and 7 mm and a width of 0.34 mm were used. To get the same energy per area applied with the top-hat, a higher average power was used. The power was limited by the spatial light modulator to 57 W for the 7 mm top-hat and 51 W for the 9 mm top-hat line. The velocity was varied from 200 to 1000 mm/s. Fig. 6 shows the quality in comparison to the energy per area. As shown before with the Gaussian beam quality rating, low energy per area (< 8 mJ/mm²) leads to a poor quality rating 1 to 3. The “good” processing window (4 to 6) seems to be in range of 10 to 13 mJ/mm². Higher energy per area leads to melted and warped results as well. Because of the fixed power, the quality variation at a fixed energy per area is not as high as the variation of the Gaussian beam profile in Fig. 5.

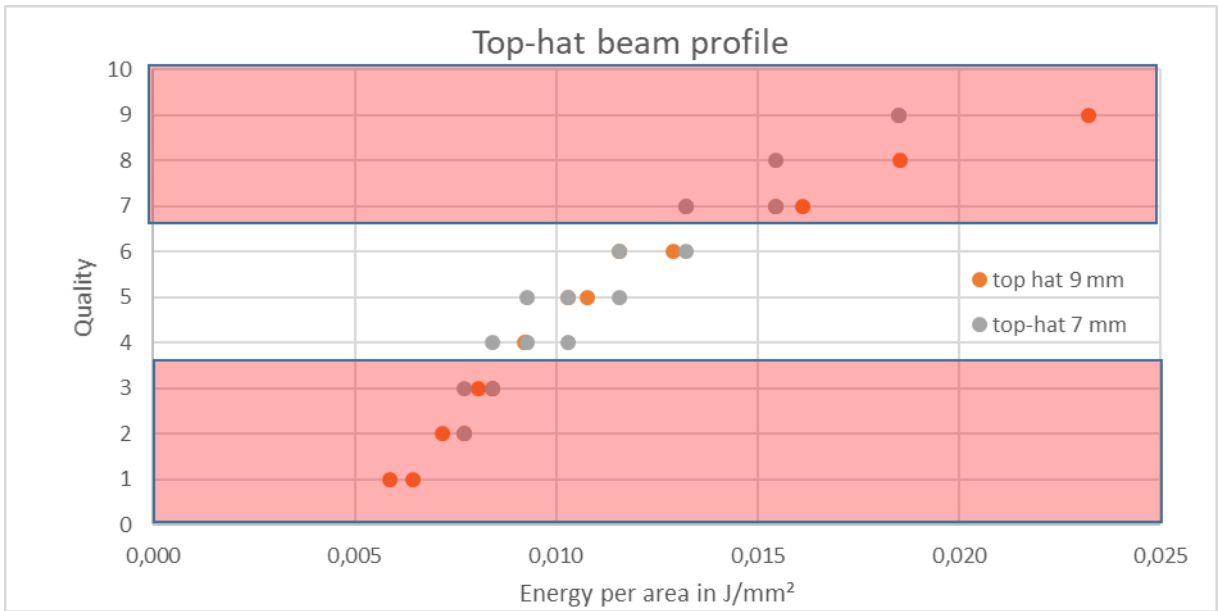

Fig. 6. *Process results top-hat: Quality over energy per area*

3.3. Influence of Intensity

Fig. 7 shows the quality in comparison to the beam intensity of the Gaussian and the top-hat beam profile. A fixed energy per area of 11 mJ/mm² is plotted. As can be seen, the quality rating increases slightly with higher intensity from the lower end of "good" quality rating 4 at 16 W/mm² to melted and warped "bad" quality and a rating of 8 at 160 W/mm². The same effect was ascertained at higher energy per area. The high local intensity seems to overheat the surface of the sintered powder. Because of the low heat conductivity, the energy does not reach the deeper powder to sinter it.

It was possible to use a much lower intensity in the range of 16 W/mm² with the 9 mm x 0.34 mm top-hat beam profile. The sintered top-hat sample with a quality of 5 is shown in Fig. 8 (left). With the same visible result, the Gaussian sample can be seen in Fig. 8 (right). Both samples have the same visible grey shade and are not warped.

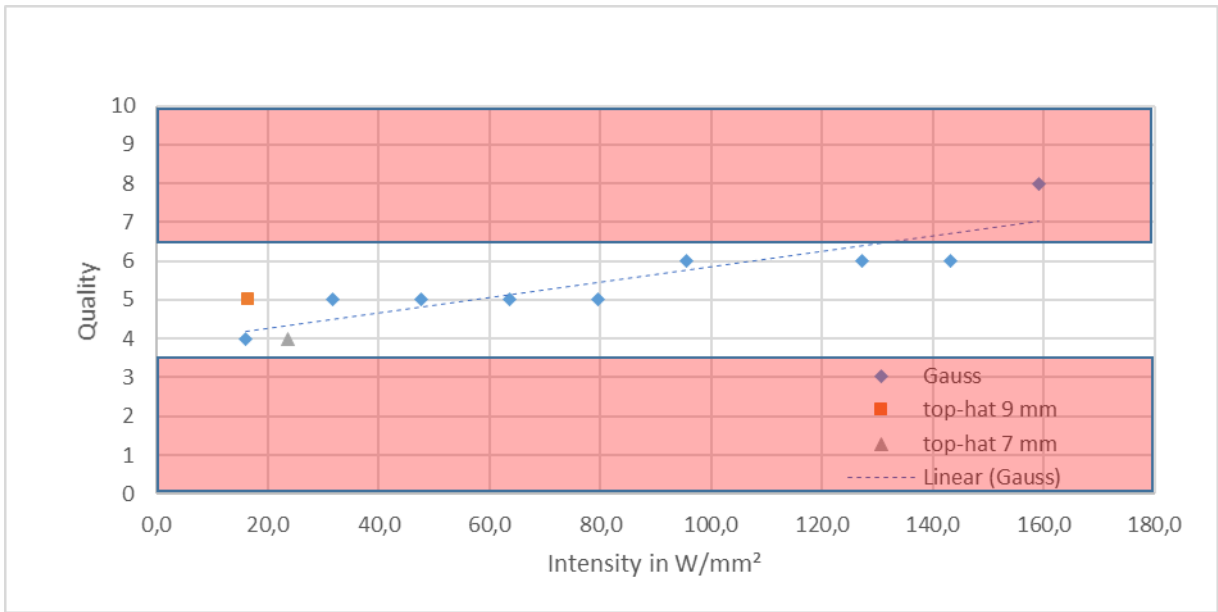

Fig. 7. *Process results: Quality over intensity at a fixed energy per area of 11 mJ/mm²*

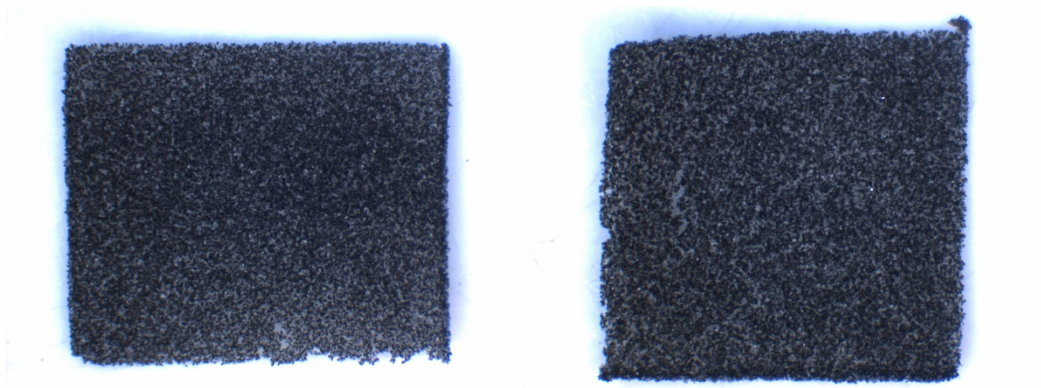

Fig. 8. *Sample: energy per area of 11 mJ/mm² (left:) top-hat 9 mm x 0.34 mm; (right): Gauss 0.4 mm*

3.4. Productivity

As defined before, the productivity of the SLS process is measured with the sintered volume per time. To demonstrate the benefits of the spatial light modulator and the shown top-hat beam profile, the thickness of each sample was measured. Depending on the energy per area, a thickness between 100 µm and 180 µm was measured for the shown parameter field. As shown before, the volume per time is calculated by the beam size, thickness and scan velocity including jump times and the acceleration time for each line. Fig. *9* shows the volume per time and the power. The parameters were selected by a “good” (5) quality result. The

diagram shows a volume per time of maximal 150 mm³/s with the 0.4 mm Gaussian beam profile at a maximum power of 18 W and a scan velocity of 9000 mm/s. The scan velocity was limited by the used galvanometer scanner. A much higher volume per time of around 900 mm³/s was achieved by the 7 mm x 0.34 mm top-hat beam profile. At a power of 56 W and a much slower velocity of 870 mm/s was used. Because of the limited jump speed of 10000 mm/s the hatching with the 0.4 mm Gaussian beam takes much longer than the top-hat beam.

As shown in Fig. *10*, two sintered rectangles of 28.8 mm x 34 mm were hatched with both parameters.

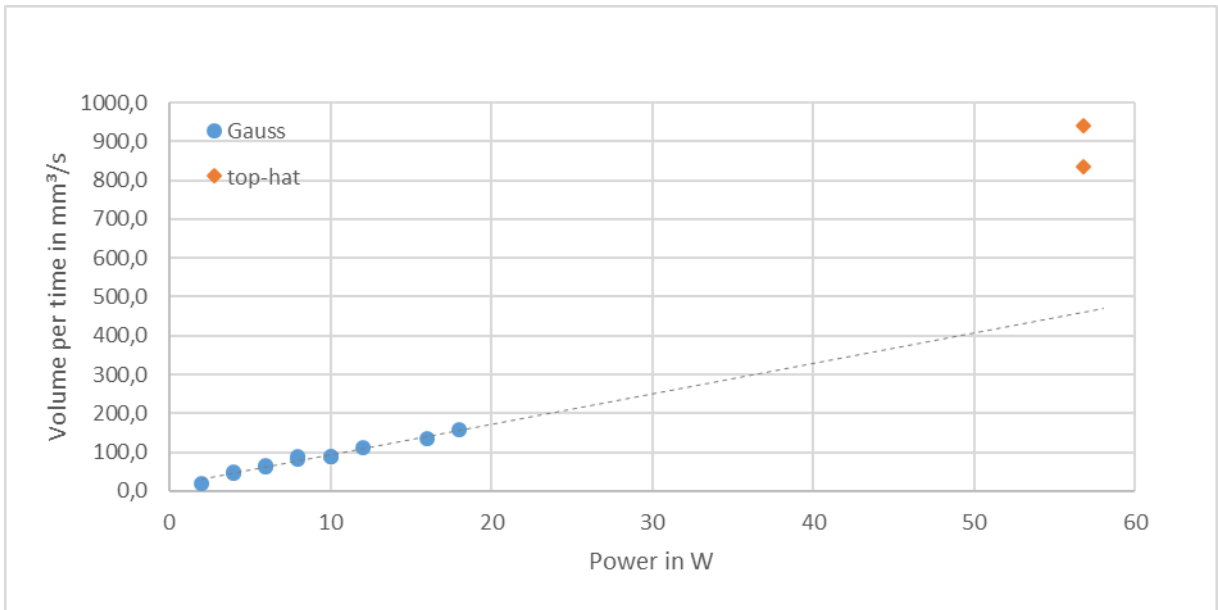

Fig. 9. *Volume per time over power: selected parameters with "good" quality (5) result*

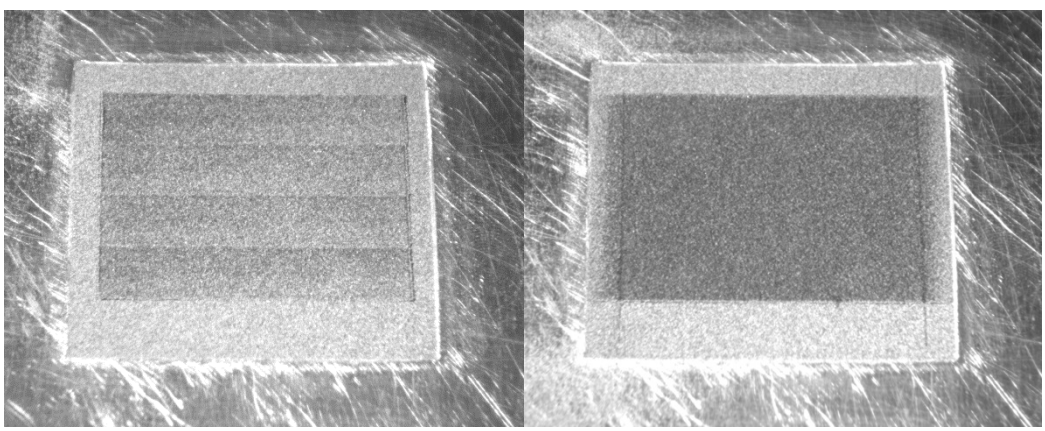

Fig. 10. *Left: 7 mm top-hat beam profile, right: 0.4 mm Gauss beam profile*

4. Conclusion

The dependence of the quality on the energy per area as well as the intensity was qualified. For the processing window, the energy per area was identified in the range of 10 to 11 mJ/mm² for a “good” quality rating. The intensity limitation in this setup at around 140 W/mm² for the Gaussian beam was detected. For the 0.4 mm beam size, the power limit was at 18 W for a velocity of 9000 mm/s. Derived from that, the top-hat profile was increased to 7 mm and 9 mm in length and 0.34 mm in width. Because of the huge size of the beam, the power could be increased to up to 56 W at a scan velocity of 870 mm/s. The productivity in form of volume per time was increased from 200 mm³/s for the Gaussian beam to about 900 mm³/s for the top-hat beam.

The laser power for the top-hat beam was only limited by the spatial light modulator. Theoretically, the power can be increased much more without loss of quality.

References

Dickey, Fred M. (Monday 2000): Laser beam shaping techniques. In: Proceedings of SPIE. High-Power Laser Ablation III. Santa Fe, NM, USA, Monday 24 April 2000: SPIE, S. 338–348.

Hopkinson, Neil; Hague, Richard J. M.; Dickens, Phill M. (Hg.) (2006): Rapid manufacturing. An industrial revolution for the digital age. [Elektronische Ressource]. Chichester: Wiley.

Paul, Ratnadeep; Anand, Sam (2012): Process energy analysis and optimization in selective laser sintering. In: *Journal of Manufacturing Systems* 31 (4), S. 429–437. DOI: 10.1016/j.jmsy.2012.07.004.

Peyre, Patrice; Rouchausse, Yann; Defauchy, Denis; Régnier, Gilles (2015): Experimental and numerical analysis of the selective laser sintering (SLS) of PA12 and PEKK semi-crystalline polymers. In: *Journal of Materials Processing Technology* 225, S. 326–336. DOI: 10.1016/j.jmatprotec.2015.04.030.